Quantitating Left Ventricular Dynamics From Single Plane Videometry*

P.D. Clayton, W.F. Bulawa, P.M. Urie, H.W. Marshall, and H.R. Warner, Salt Lake City, Utah, USA

Introduction

To understand the role which videometry plays at the LDS Hospital, a brief review of the overall catheterization system is helpful. We have established a computerized quantitative cardiology data base. The input to this data base comes from varied sources. In addition to the data which are collected routinely on most elective admissions to the hospital (self-administered patient history [Warner, Rutherford and Houtchens 1972], ECG [Pryor, Lindsay and England 1972], clinical laboratory, tonometry and spirometry [Schmidt et al. 1973]), cardiology data is also gathered from computerized ECG stress testing (Pryor and Ridges 1974), computerized catheterization measurements (Gardner and Hoecherl 1970, Warner et al. 1970), and automated analysis of left ventricular angiograms. Computer terminals are used to enter clinical data derived from history and physical examination, interpretations of selective coronary arteriograms and surgical procedure codes. With this comprehensive clinical data base, it is possible to implement automated decision making using HELP.

HELP (Pryor et al. 1975, Warner, Olmsted and Rutherford 1972) is a system for automated medical decision making in which criteria for decision making can be entered into the computer in natural language. The HELP compiler translates the natural language criteria to an efficient format for computer execution (decision sectors) and stores this logic on disk. Whenever new data is added to a patient's record, the appropriate decision sectors are executed. If the data satisfy any of the sectors, that decision is added to the patient's decision list and displayed on the cardiologist's terminal. If discrepancies between the automated decisions and the cardiologist exist, the necessary investigation to resolve the disagreement is undertaken; otherwise the HELP decisions are also printed as part of the catheterization report.

Certain diagnoses which cannot be made on the basis of hemodynamic data alone are entered at a CRT terminal in coded form using the systematized nomenclature of pathology (SNOP) (Morgan 1971). The HELP system can also be used to stratify or objectively classify patients so that attempts to quantitatively investigate the correlation between various parameters and specified disease states can be carried out with ease and versatility.

Although the computerized catheterization laboratory at LDS Hospital has been operational for over 10 years, there have been some recent changes. The gradient program now measures simultaneous pressures from two transducers. The resulting pressure waveforms can be temporarily shifted relative to each other by the cardiologist to align the onset of systole or any other fiducial marker. This compensates for the different time delays in the catheter systems and allows precise beat by beat calculation of valvular gradients even in patients with irregular cardiac rhythm. Using cardiac output and gradient measurements, mitral valve and aortic valve areas are calculated using the formulae proposed by Gorlin and Gorlin (Gorlin and Gorlin 1951). The valve areas rather than the magnitude of the gradients are used to classify valvular stenosis as mild, moderate or severe in the HELP sectors.

Videometric Methods

Along with the hemodynamic data recorded in the catheterization laboratory, quantitative description of left ventricular function is necessary. In our laboratory, ventricular function

* Supported in part from NHLI Grant #HL04664

is analyzed using a series of contours (obtained at 1/60 second intervals) representing the endocardial borders of the left ventricular chamber during systole. The ventricular borders are obtained (Clayton et al. 1974) by recording the ventriculograms on a computer controlled stop action video disk. A video digitizer computer interface is used to convert each video field to a grey level matrix in the computer. This matrix is processed line by line. The probability that each point on a line is the left or right border is calculated as the product of several terms which model the visual recognition process: a gradient matched filter, video level and location predictors (based upon values of the border points on adjacent lines), and a sequence predictor (predicted location based upon extrapolated movement from the two previous fields). Rather than using the video profile predictor mentioned in earlier reports, a software version of the Rotterdam border algorithm (DeJong and Slager 1975) has been implemented as the video level predictor.

After a sequence of left ventricular borders has been determined, quantitative parameters are derived to describe the border motion. Several alternative methods of defining the reference systems and measuring segmental wall motion have been compared in our laboratory. A radial regression model (Harris et al. 1974, Marshall et al. 1975) has been developed which compares the movement of any given wall segment against the average contraction for the entire ventricle. This is accomplished by drawing radii from the reference point (generally chosen as the mid point of the long axis of the ventricle in the RAO projection) to the endocardial border at 5° intervals. The average radial length of the 54 segments of the contour (excluding those which represent the aortic or mitral valves) is also calculated. The time sequence of radial lengths during systole for each segment is then plotted against the time sequence of the average radial length yielding 54 separate regressions (one per segment). The magnitude of the regression slope (b) quantitatively shows whether the contraction of that segment is greater ($b > 1$) or less ($b < 1$) than the average for the ventricle. A high correlation coefficient ($r \approx 1$) shows that the contraction of that segment is synchronous with that of the entire ventricle. The resulting analysis for the entire heart is then plotted to show the regression slope and correlation coefficient at each angle.

In addition to the radial model, parameters were derived using the commonly used hemidiameter model. The hemidiameter measurements refer to 72 equally spaced half diameters from the long axis of the ventricle to the endocardial wall on each side of the chamber. The first 18 hemidiameters on the inferior wall in the RAO view were excluded because they represent the region of the mitral valve. For each of the remaining 54 hemidiameters, segmental wall motion parameters were calculated by plotting the individual hemidiameter lengths against the time sequence of the average of all hemidiameters (the same method used for the radial model). The linear correlation coefficient, regression slope and percent shortening were obtained for both the radial and hemimodels giving a total of six parameters which measured segmental wall motion.

To establish the normal range for each of these 6 parameters, 53 normal patients were studied. The clinical criteria for the normal classification were 1) less than 50% obstruction in any branches of the coronary arteries, 2) no history of previous infarction, 3) no valvular dysfunction, and 4) no Q waves in the ECG. Histograms of the values of each parameter were plotted for each segment. In the case of hemi and radial correlation coefficients, a threshold (99.9% level) was established at each angle by fitting a Poisson distribution,

$$f(r) = \frac{e^{-\lambda}\lambda^{r}}{r!}$$

to a plot of the values of the correlation coefficients for the normal group. In this formula, r is the amount by which the correlation coefficient differs from one and λ is the mean value of these differences. To determine cutoffs for values of percent shortening and regression slope, the data for the normal group were fitted to a Gaussian distribution and the threshold determined at the 2.5 σ (95%) level.

After the limits for normal hearts were established, the ability of each parameter to distinguish between normal and abnormal was tested. Thirty-five patients with clinical evidence of fibrosis (Q waves in the ECG) were studied and a histogram was constructed for each of the six parameters. The hisotograms (see Fig. 1 for example) show the number of con-

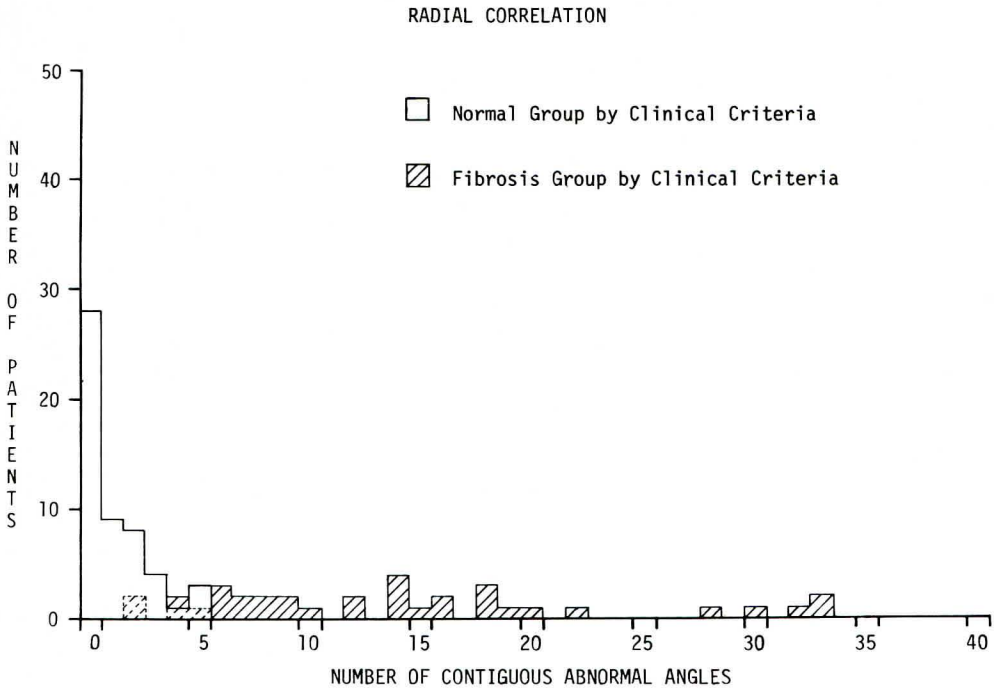

Fig. 1 Histogram of the number of contiguous abnormal angles for the radial correlation parameter for the normal and fibrotic populations. Any ventricle with 6 or more contiguous abnormal segments would be classified as fibrotic using this parameter

tiguous abnormal (parameter value below the normal threshold) segments for both normal and abnormal hearts. The cutoff was chosen to minimize the misclassification of normals and maximize separation of the two groups.

The sequence of ventricular contours during systole is also used to extract information about the phase relationships between the contracting segments. Theoretical considerations indicate that phase information may be used to differentiate ischemic myocardial segments from nonrecoverable scar tissue. It was shown. (Tyberg et al. 1970, Tyberg et al. 1969, Banka and Helfant 1974) that isolated cat papillary muscles under hypoxic conditions exhibited asynchrony or phase differences when compared to normal muscle. During hypoxia, the developed tension, the time from stimulus to peak tension, and the time for tension to decay to one-half its peak tension all decreased dramatically from normal values. At the onset of contraction, the motion of hypoxic and normal muscle is the same. However, soon after the beginning of contraction, the hypoxic muscle develops its peak tension and starts to relax while the tension in the normal muscle continues to increase. Therefore, one might expect that the regression of the radial distances to the hypoxic segments of the ventricle against the average radius would yield a curve which is concave upward (positive curvature).

In contrast, fibrotic tissue, which does not develop active tension, acts as a passive segment of the ventricular wall and its motion is determined by surrounding muscle tissue. Consequently, one might expect the motion of fibrotic tissue to be delayed until later in systole compared to surrounding muscle tissue. This delay would yield a curve which is concave downward (negative curvature) when the motion of fibrotic tissue is plotted against the motion of normal tissue.
Additional observations revealed that in recently reoxygenated hypoxic muscle, the time to peak tension and the time for tension to decay to one-helf of peak tension was greatly

prolonged over normal values. This delay in the onset of peak tension in recently reoxygenated hypoxic muscles would also yield a curve which is concave downward (negative curvature).

In order to quantitate such a relationship in which there is curvature or a phase difference, a least squares method was used to fit a parabola to the data. To do this, the origin of the coordinate system was translated to the point on the regression line which is the midpoint of the average radius sequence. The coordinate axes were then rotated so that the linear regression line becomes the x axis (Fig. 2). This makes the axis of symmetry of the parabola parallel to the y axis. A least squares method is used to fit a parabola of the form ($f(x) = ax^2 + bx + c$) to the data. The coefficient of the linear term (b) is very close to zero because of the rotation and translation of the coordinate axes and thus was neglected. The coefficient of the quadratic term (a) is a measure of the amount of curvature of the parabola and the sign of the term indicates whether the parabola is concave upward (positive) or concave downward (negative). This coefficient is referred to as the curvature value and is a quantitative measure of phase differences in the segmental wall motion. Curvature values were calculated over all angles in the 53 normal and 35 fibrotic cases. In addition 25 patients with substantial coronary artery disease (greater than 75% occlusion) and no previous documented myocardial infarction were studied.

To investigate the validity of the curvature values, an independent method was used to study the phase patterns in the normal group. The time (t) of onset of contraction for each segment was calculated by finding the video field in which the hemidiameter for that segment reached maximum length. This time was compared to the time (t_o) of end-diastole (the field with maximum ventricular volume) to see if the onset of contraction in each segment leads or lags the average contraction of the ventricle. This time difference was used as a parameter to examine the onset of contraction and was calculated for each segment in 23 normal RAO ventriculograms and 8 LAO ventriculograms.

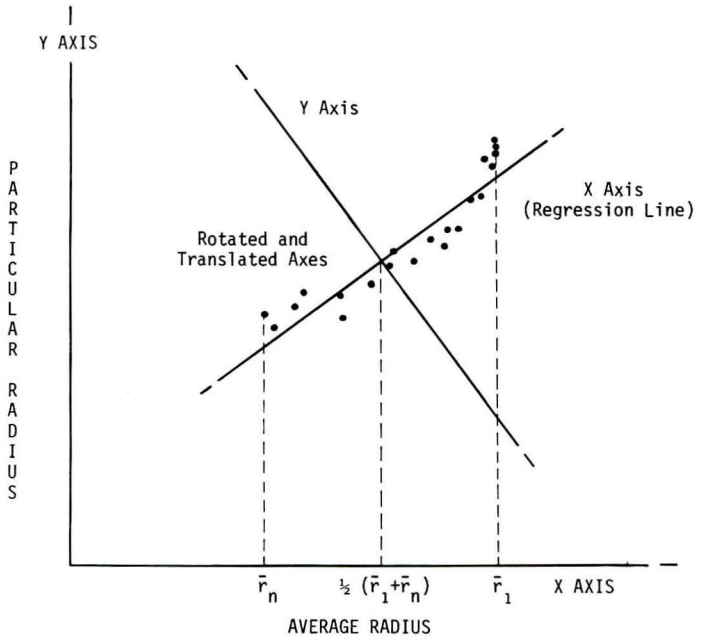

Fig. 2 The radial length for a given segment plotted against the average radial length. The axes are translated and rotated for a curvature calculation

Results

The border algorithm performance is really a measure of two processes. First, accurate determination of the ventricular contour and second, automatic identification of the three points (left base, right base, apex) which define the reference point (mid point of the long axis of the ventricle).

Evaluation of border algorithm success is done in various ways. Whenever the operator must make hand corrections to a computer determined border, the manually entered points are flagged as they are stored in the border contour. In the analysis of all fields during a single systole in 7 patients, taken as they came through the catheterization laboratory, 25% of all border points were manually corrected by the operator.

During January, February and March of 1976, 206 RAO ventriculograms (412 end-diastolic and end-systolic contours) were processed as a routine clinical service. Without the sequence term, 15% (63/412) of the borders were completely computer determined. When the sequence mode was used, an additional 43% (177/412) of the contours were accurately found by the computer. Acceptable contours were obtained by manually correcting portions of 54 of the remaining contours (13% of the total); and ultimately, 29% (118/412) were completely hand traced.

Ventricular volumes and ejection fractions are calculated using Simpson's Rule (Davila and Sanmarco 1966). The use of this rule is somewhat unique, however, in that 144 hemidiameters are used to slice the ventricle normal to the long axis rather than generate the conventional horizontal slices. There was good agreement between this method and the area-length model (Dodge et al. 1960). Table 1 summarizes the results of this comparison in 762 patients. According to this comparison,the area-length method for end-systole is as accurate as it is for end-diastole. This is noteworthy because the ventricle at end-systole does not seem to approximate the ellipse upon which the area-length method is modeled.

Table 1 Comparison of Simpson's rule (sections normal to long axis of ventricle) with the area-length method for computing ventricular volume

	n	Correlation Coefficient	Regression Slope	Intercept	Standard Error of Estimate (Measure of Scatter)
Ejection fraction	762	0.992	1.019 ± .0002	−.02	.02
End-diastolic volume	742	0.996	.985 ± .0001	.4 ml	6.67 ml
End-systolic volume	742	0.987	.995 ± .0002	.8 ml	9.12 ml
Stroke volume	765	0.976	.977 ± .0003	−.2 ml	10.4 ml

The thresholds for normal values of the various parameters are plotted in Fig. 3. The high correlation coefficients show that normal ventricular contraction as visualized in the RAO projection is highly synchronous. The thresholds are slightly lower on the inferior wall than the anterior wall. The ability of the various parameters to separate normal from abnormal motion is given in Table 2. The success ratio for each parameter is remarkably high when one considers that these results come from single plane 30° RAO angiograms with projections which are not expected to totally visualize certain infarcts.

The averaged curvature for the normal patients is shown in Fig. 4. Although the variance is relatively large, the trend of the means is significant ($p < .01$) when analyzed with a "t" test. A Kolmogorov-Smirnov test was used to show that the distributions of values about the means at each angle were not significantly different from normal distributions. Therefore, the trend shows positive curvature (lead) on the inferior wall and negative curvature (lag) at the apex, and does not appear to be caused by a small number of individuals whose values are abnormal.

The mean values of the time lead or lag (hemidiameter onset of contraction model) are shown in Fig. 5. Again the variation is large, but the trend is significant. The inferior wall generally contracts 1 field (16 ms) earlier than the average for the ventricle, the apex lags by approximately 1 1/2 fields (24 ms) and the anterior wall, except toward the base, ge-

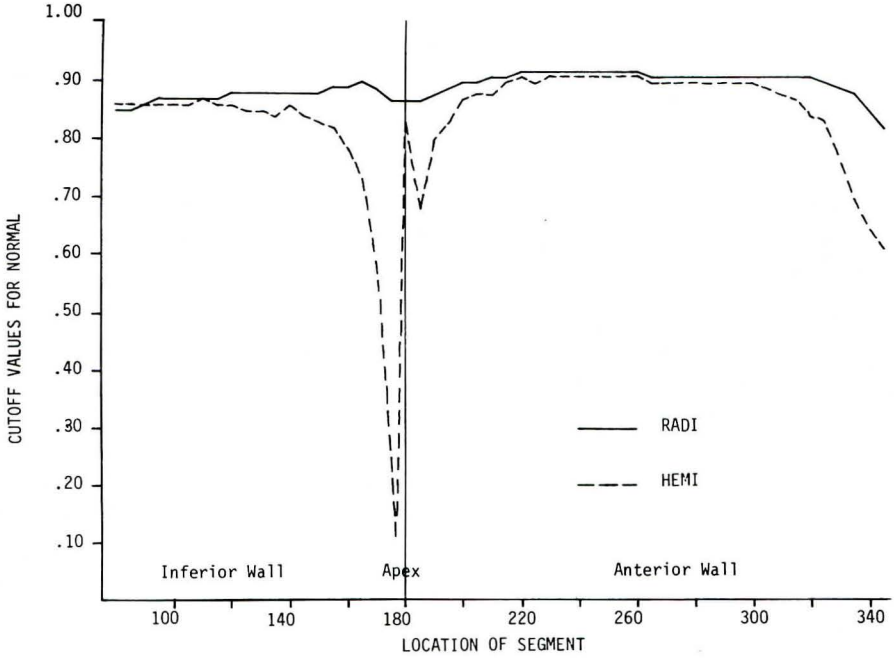

Fig. 3a

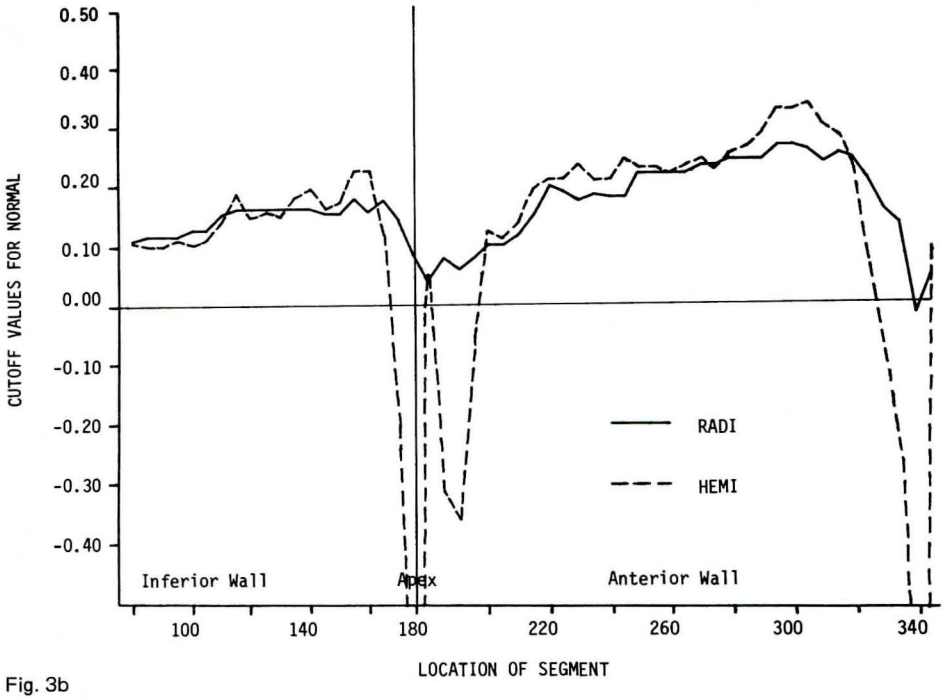

Fig. 3b

Fig. 3 Normal population threshold values for (a) correlation coefficients, (b) percent shortening and (c) regression slopes

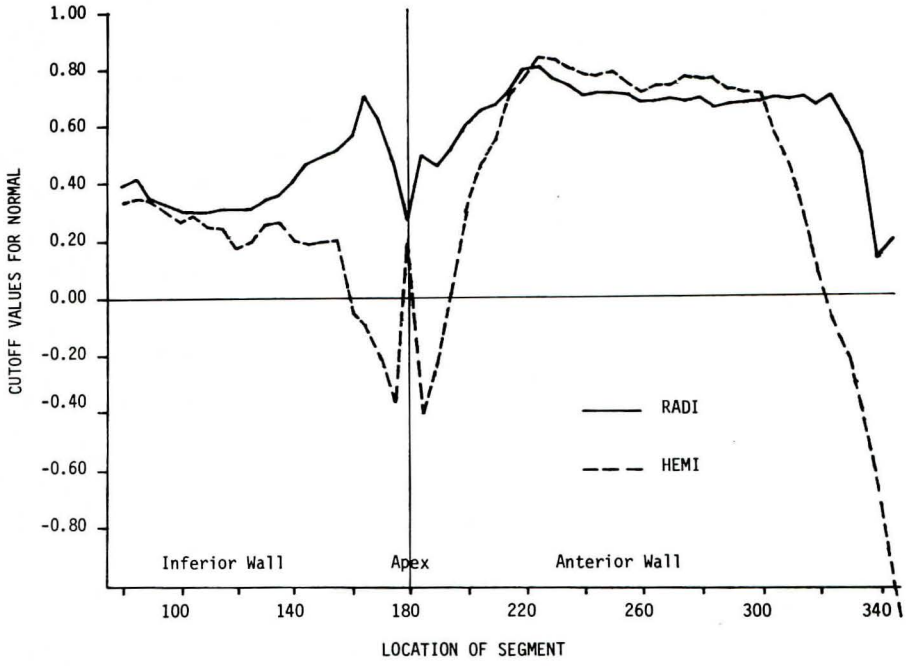

Fig. 3c

Table 2 A summary of the accuracy of various quantitative methods for separating normals from abnormals

	Radial Correlation	Percent of Radial Shortening	Hemi-correlation	Radial Regression	Percent of Hemi-shortening	Hemi-regression
Missed normals	0/53	2/53	1/53	1/53	3/53	6/53
Missed fibrosis	5/35	4/35	5/35	5/35	4/35	3/35
Threshold number of contiguous angles in an abnormal segment	6	1	9	4	3	2
Percent correct classification	94.3%	93.1%	93.1%	93.1%	92.0%	89.7%

nerally reflects the average for the ventricle. This pattern corroborates the curvature findings in that, if the inferior wall starts to contract while the average radius is not changing, the resulting regression slope will exhibit positive curvature. Similarly if the apex hemidiameters are not contracting as early as the rest of the ventricle the resulting curvature will be negative. If the curvature graph of Fig. 4 is inverted and compared to the sequence of the onset of contraction in Fig. 5, the agreement (Fig. 6) is striking. This agreement is even more striking when one considers that the curvature values were computed for the radial model using automated border recognition and the time lead and lag values were computed

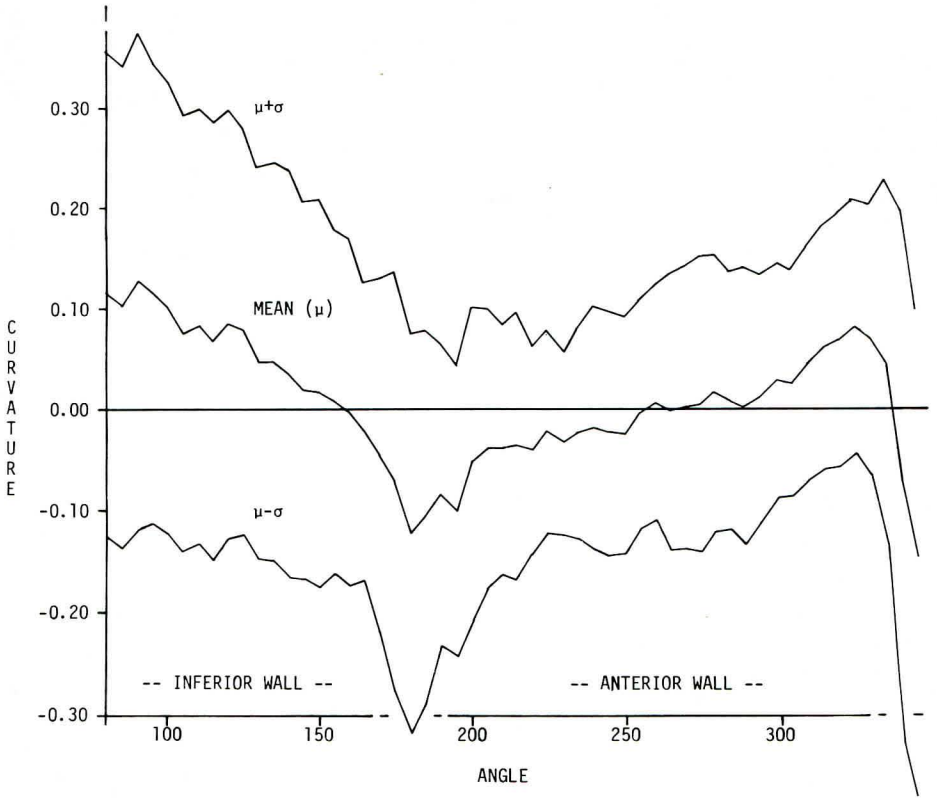

Fig. 4 The mean and standard deviation of curvature values in the RAO view for the normal patient population vs. angle

using hemidiameters on hand traced contours. In 8 patients with LAO angiograms, the averaged response showed the onset of contraction to begin at the apex and move toward the base along the posterolateral wall.

A histogram of the curvature values for all segments which fell below the normal threshold in fibrotic (35 patients with Q waves) and hypoxic (25 patients with significant coronary artery disease but no Q waves) groups is shown in Fig. 7. The curvature method was not effective in separating hypoxic from fibrotic myocardium.

Summary

Problems in ventricular border recognition are inherent in the visual process also. The border at end-diastole is more easily visualized because the myocardium is stretched. As systole proceeds, the effects of trabeculation become more pronounced and the "border" becomes in actuality a result of superimposition of several borders. Toward end-systole there is often a false impression of movement as dye is expelled from the irregular fissures in the endocardium. These types of "pseudocontraction" are an important source of noise in the phase investigations discussed in this article.

The high degree of success which each parameter demonstrates in separating normal from abnormal (previous MI) ventricles indicates that the reference point system may not be as critical as some have suggested. In view of the increased work necessary to generate multiple contours, it is interesting that the radial percent of shortening method (which uses only end-diastolic and end-systolic contours) compares very favorably with other methods. The range in normal values for the radial correlation coefficient is much less than for any of the

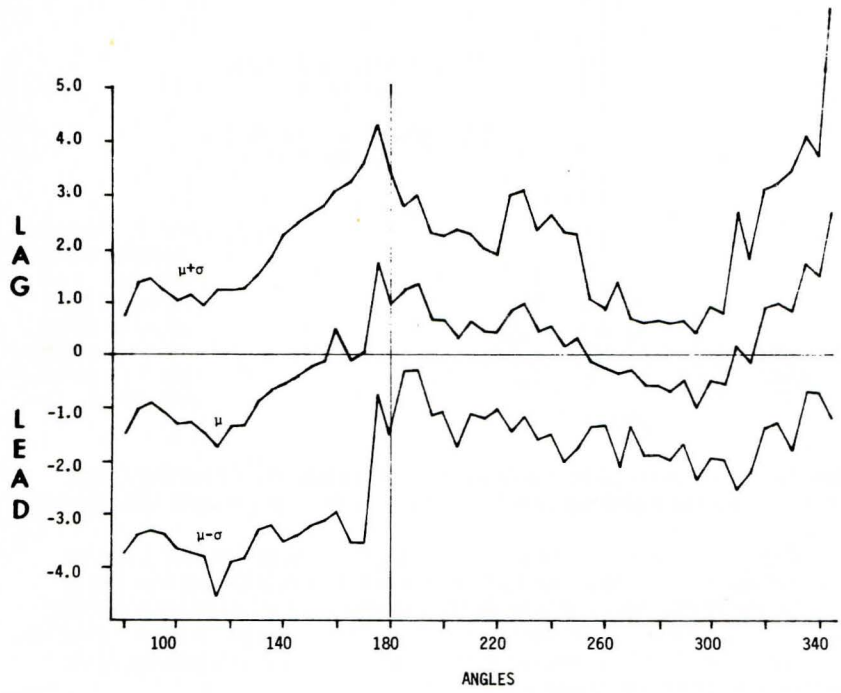

Fig. 5 The mean and standard deviation of the onset of contraction values. The units of lead and lag for the verticle axis correspond to one video field (1/60 sec.)

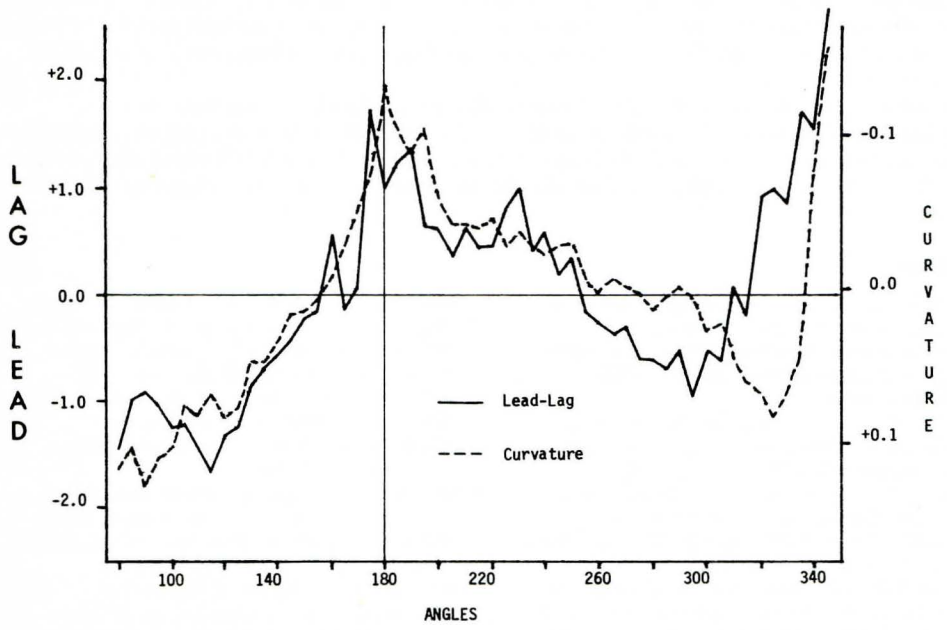

Fig. 6 A comparison of the normal activation sequence in RAO ventriculograms as determined by the curvature and onset of contraction methods. The units are the same as in Fig. 4 and 5

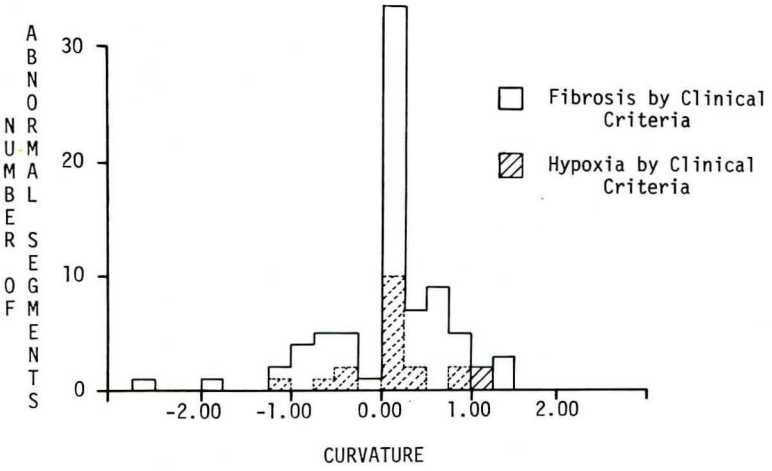

Fig. 7 Histrogram showing the distribution of curvature values for those segments whose correlation coefficients fell below the normal threshold

other parameters and this appears to be the most sensitive parameter. From the graphs in Fig. 3, it is evident that the radial parameters are more reliable at the apex than the hemidiameter parameters.

Measurement of phase in the normal ventricle shows an „antimilking" motion (the mid ventricle begins to contact earlier than the apex) in the RAO view. The fact that the inferior wall leads the rest of the ventricle may be the explanation for the reduced correlation coefficient thresholds found in the normal ventricle. The close agreement between the curvature values and the lead and lag measurements tends to support the validity of the indicated sequence of ventricular contraction.

Assuming that the curvature hypothesis is correct, there are several possible explanations for the lack of success in separating fibrotic from ischemic ventricles. In the fibrotic group, the single plane angiogram will not always project the actual infarct on the edge of the silhouette but may involve ischemic muscle surrounding the scar. In the "ischemic" group with coronary artery disease, the incidence of angina during the procedures was low. Therefore, this group might not be expected to generate strong phase differences in contraction at the time of the study.

In summary, an automated system for ventricular border detection and parameter extraction has been developed. A classification system has been implemented using an automated decision making system (HELP). This allows integration of dynamic left ventricular geometrical data with hemodynamic and clinical data for patient management using explicit algorithms.

References

Banka, V.S., R.H. Helfant: Temporal sequence of dynamic contractile characteristics in ischemic and nonischemic myocardium after acute coronary ligation. Amer. J. Card. 34:158, 1974

Clayton, P.D., L.D. Harris, S.R. Rumel, H.R. Warner: Left ventricular videometry. Comp. and Biomed. Res. 7:369-379, 1974

Davila, J.D., M.E. Sanmarco: An analysis of the fit of mathematical models applicable to the measurement of left ventricular volume. Am. J. Card. 18:31-42, 1966

DeJong, L.P., C.J. Slager: Automatic detection of the left ventricular outline in angiographs using television signal processing techniques. IEEE Trans. Biomed. Eng. BME 20:230-237, May 1975

Dodge, H.T., H. Sandler, D.W. Ballew, J.D. Lord Jr.: The use of biplane angiocardiography for the measurement of left ventricular volume in Man. Am. Heart J. 60:762-776, 1960

Gardner, R.M., A.W. Hoecherl: Instrumentation for computerized heart catheterization. IEEE Transactions on Biomedical Engineering 18:60-65, 1970

Gorlin, R., S.G. Gorlin: Hydraulic formula for calculation of the area of the stenotic mitral valve, other cardiac valves, and central circulatory shunts. Am. Heart J., 41;1, 1951

Harris, L.D., P.D. Clayton, H.W. Marshall, H.R. Warner: A technique for the detection of asynergistic motion of the left ventricle. Comp. and Biomed.Res. 7:380, 1974

Marshall, H.W., P.D. Clayton, P.M. Urie, H.R. Warner, H.V. Liddle: Assessment of ventricular function in coronary artery disease using nitroglycerin and computerized analysis of left ventriculograms. Ann. Thor. Surg. Vol. 20, No. 2:127-135, August 1975

Morgan, J.D.: A Computerized „Conversational" Technique to form numerically coded medical diagnoses, PhD Thesis University of Utah, June 1971 (unpublished)

Pryor, T.A., A.E. Lindsay, R.W. England: Computer analysis of serial electrocardiograms. Comp. and Biomed. Res. 5:709-714, 1972

Pryor, T.A., D.J. Ridges: A computer program for stress test data processing. Comp. and Biomed. Res. 7:360-368, 1974

Pryor, T.A., J.D. Morgan, S.J. Clark, W.A. Miller, H.R. Warner: HELP–A computer system for medical decision making. Computer 34, 1975

Schmidt, D.E., M.L. Dickman, R.M. Gardner, F.K. Brough: Spirometric standards for healthy elderly men and women. Am. Rev. Resp. Dis. 108:933-939, 1973

Tyberg, J.V., L.A. Yeatman, W.W. Parmley, C.W. Urschel, E.H. Sonnenblick: Effects of hypoxia on mechanics of cardiac contraction. Am. J. Physiol. 218:1780, 1970

Tyberg, J.V., W.W. Parmley, E.H. Sonnenblick: In vitro studies of myocardial asynchrony and regional hypoxia. Circ. Res. 25:569-579, 1969

Warner, H.R., B.D. Rutherford, B. Houtchens: A sequential Bayesean approach to history taking and diagnosis. Comp. and Biomed. Res. 5:256-262, 1972

Warner, H.R., R.M. Gardner, T.A. Pryor, W.C. Day, W.M. Stauffer: A system for on-line computer analysis of data during heart catheterization in pathophysiology of congenital heart disease, Univ. of Calif. Press. Berkeley & Los Angeles. pp. 409-418, ed. by F.H. Adams, H.J. C. Swan, V.E. Hall, 1970

Warner, H.R., C.M. Olmsted, B.D. Rutherford: HELP – A program for medical decision making. Comp. and Biomed. Res. 5:65-74, 1972

Roentgen-Video-Techniques

117

for Dynamic Studies of Structure and Function of the Heart and Circulation

2nd International Workshop Conference, April 1976

Edited by
P. H. Heintzen and J. H. Bürsch

With Contributions by

L. Björk
R. Brennecke
A. B. Brill
T. K. Brown
J. H. Bürsch
W. F. Bulawa
J. H. Chesebro
P. A. Chevalier
A. Chu
D. Clayton
J. J. Ericson
U. Erikson
Ch. Faltz
F. L. Farr
M. Felgendreher
R. L. Frye
H. Garten
B. K. Gilbert
P. Gildberg
T. P. Graham
J. Grimm
W. Harlander
L. D. Harris
P. H. Heintzen
G. T. Herman
H. Huber
J. Huebel
G. Hüttig
R. Johs
Dan Kedem
Drora Kedem
A. Kléber
P. Lange
B. Lantz
B. Lindberg
D. P. Lindstrom
V. Malerczyk
H. W. Marshall
G. T. Meester
F. L. Meyler
K. Moldenhauer
J. H. Nelson
K. L. Neuhaus
D. Onnasch
J. Ostermeyer
Y. C. Pao
J. Pilarczyk
R. R. Price
J. H. C. Reiber
A. Reimann
T. C. Rhea
E. L. Ritman
R. A. Robb
S. W. Rowland
P. E. Ruegsegger
G. Ruhn
W. Rutishauser
F. K. Schmiel
J. C. H. Schuurbiers
U. Sigwart
N. R. Silverman
R. Simon
C. J. Slager
C. W. Smith
H. C. Smith
J. H. J. Sneek
W. Spiesberger
P. Spiller
E. Stelzer
E. Stephan
B. Straume
R. E. Sturm
M. Tasto
G. Trieb
P. M. Urie
H. R. Warner
A. Wessel
R. P. van Wijk van Brievingh
M. Wolgast
E. H. Wood
K. Ziegler

273 Figures, 17 Tables

Georg Thieme Publishers Stuttgart 1978